RSC Advances

PAPER

View Article Online
View Journal | View Issue

Cite this: *RSC Adv.*, 2025, **15**, 45573

Coastal halophyte plant *Atriplex maximowicziana* with previously undescribed terpenoids and anti-colorectal cancer chlorophyll stereoisomers utilizing a molecular networking approach

Andrea Gu,[ab] Po-Jen Chen,[cd] Yih-Fung Chen,[e] Ho-Cheng Wu *[bfg] and Tzong-Huei Lee*[a]

Coastal halophyte plants are well known for producing various bioactive secondary metabolites. *Atriplex maximowicziana* Makino (Hae-Fwu-Rong), a halophyte plant growing in coastal areas of East Asia, has been traditionally used to treat pathogenic wind and rheumatoid arthritis. A comprehensive feature-based molecular networking (FBMN) analysis of fractions derived from *n*-hexane and *n*-butanol layers of *A. maximowicziana* methanolic extract revealed triterpenoids, triterpenoid saponins, and tetrapyrroles as the predominant molecular families. Guided by the prominent molecular families identified, targeted fractionation led to the isolation and structural elucidation of eight previously undescribed metabolites, including four triterpenoid-saponins, atriplexosaponins A–D (**1–4**), two triterpenoids, atriplexoterpenes A–B (**5–6**), two chlorophylls, atriplexophylls A–B (**7–8**), along with 13 known compounds (**9–21**). Eighteen compounds with sufficient amounts were evaluated for their anticancer activity on human colorectal cancer cell lines, HT-29 and HCT-116, respectively. Among them, atriplexophyll A (**7**) was the most potent against colorectal cancer cells (IC_{50} = 0.14–0.33 μM across HCT-116 and HT-29), followed by atriplexophyll B (**8**) (IC_{50} = 7.95–8.81 μM). Both showed minimal effects on normal epithelial (IEC-6) and fibroblast (3T3-L1) cells within the tested concentration range. These findings highlight the potential of chlorophyll-*b*-type compounds bearing a pyran ring as selective anticancer agents and underscore the utility of FBMN in the discovery of bioactive natural products. Altogether, these findings unveiled the potential of *A. maximowicziana* in developing therapeutics for colorectal cancer.

Received 25th August 2025
Accepted 13th November 2025

DOI: 10.1039/d5ra06325f

rsc.li/rsc-advances

Introduction

Coastal halophyte plants grow in extreme environments, evolving diverse morphological, anatomical, and physiological adaptations to endure saline conditions.[1–3] Halophyte plants typically adapt by synthesizing various secondary metabolites to counter environmental stressors like oxidative stress and high salinity.[4] Those secondary metabolites from halophytes have been illustrated to serve physiological activities with antivirus,[5] antidiabetic,[6] and antioxidant effects.[7] Additionally, they have been identified as promising renewable natural resources for cancer prevention and treatment.[7,8]

Atriplex (Amaranthaceae family), one of the halophyte plants, comprises approximately 300 species distributed across various regions, including Asia, North America, Australia, and Africa.[9] These plants are known for adapting to extreme environments, particularly saline and arid regions.[10] So far, only seven *Atriplex* species have been studied for their secondary metabolites and bioactivities, including *A. stocksii*,[11] *A. glauca* var. *ifiniensis*,[12] *A. dimorphostagia*,[13] *A. lasiantha*,[9] *A. semibaccata*,[14] *A. littoralis*,[10] and *A. halimus*.[7] Several types of phytochemicals have been isolated from *Atriplex*, including alkaloids, coumarins, flavonoids, lignanamides, and mainly terpenoids.[14] Some compounds from *Atriplex* species have shown promising activity in different bioassay platforms. For example, flavonoids have shown antioxidant and anti-inflammatory activities,[10] alkaloids and triterpenoids showed cytotoxicity.[9] *A. maximowicziana* Makino, also known as Hae-Fwu-Rong, is widely distributed along the sandy and coral-rocky seashores of East Asia.[15] The

[a]*Institute of Fisheries Science, College of Life Science, National Taiwan University, Taipei 106319, Taiwan. E-mail: thlee1@ntu.edu.tw*
[b]*School of Pharmacy, College of Pharmacy, Kaohsiung Medical University, Kaohsiung 807378, Taiwan. E-mail: hcwu@kmu.edu.tw*
[c]*Department of Pharmacology, School of Medicine, College of Medicine, Kaohsiung Medical University, Kaohsiung 807378, Taiwan*
[d]*Graduate Institute of Medicine, College of Medicine, Kaohsiung Medical University, Kaohsiung 807378, Taiwan*
[e]*Graduate Institute of Natural Products, College of Pharmacy, Kaohsiung Medical University, Kaohsiung 807378, Taiwan*
[f]*Department of Medical Research, Kaohsiung Medical University Hospital, Kaohsiung 807378, Taiwan*
[g]*Drug Development and Value Creation Research Center, Kaohsiung Medical University, Kaohsiung 807378, Taiwan*

entire plant has traditionally been used in folk medicine to expel pathogenic wind and treat rheumatoid arthritis.[16] Besides, as a halophyte, *A. maximowicziana* may produce unique stress-induced secondary metabolites that confer resilience to harsh environments.[9,10] By contrast, *A. maximowicziana* remains largely unexplored, with no published data on its chemical composition or bioactivity. Here, we provide the first chemical and biological characterization of *A. maximowicziana*, disclose six terpenoids that differ from those described in other *Atriplex* species, and demonstrate selective cytotoxicity against colorectal cancer cells. These findings broaden the chemical space currently attributed to the genus.

Molecular networking (MN), initially developed through the web-based platform global natural products social molecular networking (GNPS),[17] is a visualized computational approach for classifying metabolites based on the similarities of their MS/MS spectra.[18] Nodes within a molecular network can be annotated by comparing against compound libraries such as those in GNPS, calculating molecular formulas and MS/MS fragmentation patterns using software like SIRIUS,[19] and applying chemical classification tools such as NPClassifier[20] and ClassyFire.[21] Feature-based MN (FBMN) is an advanced version of MN that allows for the distinction of isomeric compounds.[22] This approach enables the construction of a detailed chemical map of *A. maximowicziana*, integrating classification, annotation, and dereplication to highlight interesting compounds within complex extractions. Given its potential to uncover previously undescribed bioactive constituents, further research on *A. maximowicziana* is warranted to elucidate its phytochemical and pharmacological significance.

Colorectal cancer (CRC) is one of the most prevalent and lethal malignancies worldwide, ranking as the third most commonly diagnosed cancer and the second leading cause of cancer-related deaths globally.[23] Due to the introduction of modern lifestyle (dietary habits, sedentary lifestyles, and genetic predisposition), the incidence of colorectal cancer has been steadily rising, especially in developed countries.[24] Currently, surgery and chemotherapy have served as the primary treatments for colorectal cancer. However, these approaches have notable challenges and limitations that can significantly impact patients' lives.[25] Therefore, finding drugs with high therapeutic efficiency with low side effects is essential. Natural products derived from medicinal plants and microorganisms have been a crucial source of anticancer compounds.[26] To evaluate the potential of secondary metabolites as anticancer agents, *in vitro* studies using well-established human colorectal cancer cell lines are required.[27] HCT-116 and HT-29 are widely used human colorectal cancer cell lines that serve as valuable models for drug screening and mechanistic studies.[28] By leveraging these two cell lines, our research aims to identify and characterize secondary metabolites that demonstrate the anticancer effects of the whole plant of *A. maximowicziana* against colorectal cancer.

Experimental

General experimental procedures

^{1}H, ^{13}C, 1D, and 2D nuclear magnetic resonance (NMR) spectra were acquired on an Agilent DD2 600 MHz NMR (Agilent, Santa Clara, CA, USA) and Bruker AVIII 800 MHz NMR with Cryoprobe (Bruker, Bremen, Germany). High-resolution mass spectrometry (MS) and MS/MS data were obtained using Thermo Dionex UltiMate 3000 ultra-high-performance liquid chromatography (UHPLC) coupled to a Thermo Q-Exactive Plus Orbitrap mass spectrometer system (Thermo, Waltham, MA, USA) and Thermo Dionex UltiMate 3000 UHPLC coupled to a Thermo Orbitrap Fusion Lumos Tribrid Mass Spectrometer system (Thermo, Waltham, MA, USA). Ultraviolet (UV) spectra were respectively measured on a Jasco P-2000 polarimeter (Jasco, Tokyo, Japan) and a Thermo UV-Visible Helios α spectrophotometer (Thermo, Waltham, MA, USA). Infrared (IR) spectra were recorded on a Jasco FT/IR 4100 spectrometer and a Jasco FT/IR-4600 spectrometer (Jasco, Tokyo, Japan). TLC was performed using silica gel 60 F_{254} plates and silica gel 60 RP-18 F_{254} plates with a thickness of 0.2 mm (Merck, Darmstadt, Germany). Flash medium-performance liquid chromatography (Flash-MPLC) was performed using Santai SepabeanTM machine 2 (Santai, Changzhou, China) with silica gel (SiliaFlash® P60, 230-400 mesh; Silicycle, Quebec, Canada). MPLC was carried out with glass columns packed with silica gel (Chromatorex SMB 100-20/45, Fuji Silysia Chemical, Nagoya, Japan) and RP-C18 (YMC ODS-A-HG, 12 nm, S-50, Kyoto, Japan), performed using a Waters 515 HPLC Pump (Waters, Milford, MA, USA). Diaion (Mitsubishi Chemical, Tokyo, Japan) was used for open column chromatography. Further purification steps were performed by high-performance liquid chromatography (HPLC) using the Shimadzu SCL-40 system with an SPD-M40 photodiode array (PDA) detector (Shimadzu, Kyoto, Japan).

Plant material

The whole plant of *Atriplex maximowicziana* Makino (Chenopodiaceae) was collected in February 2023 on the sandy beach of Wanggong Harbor, Changhua County, Taiwan, and identified by Dr Ho-Cheng Wu. A voucher specimen (HCW-P21) was deposited with the herbarium of the College of Pharmacy, Kaohsiung Medical University, Kaohsiung, Taiwan.

Feature-based molecular networking (FBMN) of *A. maximowicziana* fractions

The MS and MS/MS data of 11 fractions derived from the *n*-hexane and *n*-butanol layers of *A. maximowicziana* methanolic extract were obtained from Thermo DIONEX UltiMate 3000 UHPLC coupled to a Thermo Q-Exactive Focus Orbitrap mass spectrometer spectrometric system (Thermo, Waltham, MA, USA). The fractions were dissolved in methanol and filtered through 0.2 μm PTFE syringe filters (Pall, NY, USA). The analysis parameters were as follows: Thermo Hypersil GOLD™ RP-C18 UHPLC column, H_2O/95% acetonitrile 95/5 to 0/100 with 0.1% formic acid and 2 mM ammonium formate, the top three precursor ions were fragmented with ramping of energies of 10, 20, and 40 eV. The collected MS and MS/MS data were converted to mzML format by MSConvert software,[29] processed by MZmine software (ver.4),[30] then exported for FBMN analysis[22] in the GNPS platform,[17] and also output for feature structure annotation, prediction, and classification with NP Classifier,[20]

ClassyFire[21] by software SIRIUS (ver.6).[19] The FBMN network on GNPS was generated in the linkages between nodes with cosine scores above 0.7, and at least six matched fragment ions (job ID: 8e1a1e1a47a746c48321b479e2eb8281). The GNPS library was utilized for node annotation, with at least six matching peaks and cosine scores above 0.7.

Extraction and isolation

The dried *A. maximowicziana* (12.8 kg) was extracted at room temperature with methanol (MeOH) (70 L) three times to yield a MeOH extract (1.6 kg). The MeOH extract was partitioned between *n*-hexane (Hex) and H_2O (1 : 1) to yield a Hex-soluble layer (124.9 g) and an H_2O-soluble layer. Then, the H_2O-soluble layer was partitioned between *n*-butanol (BuOH) and H_2O (1 : 1) to yield a BuOH-soluble layer (97.8 g) and an H_2O-soluble layer (202.2 g). The Hex-soluble layer (124.9 g) was subjected to Flash-MPLC (silica gel; *n*-hexane/ethyl acetate 90/10 to 100% ethyl acetate, then washed with 100% methanol) to produce seven fractions (Fr. 1–7). The BuOH-soluble layer (97.8 g) was subjected to column chromatography (Diaion; water/methanol 75/25 to 100% methanol, then washed with 100% acetone) to yield four fractions (Fr. 8–11). Fr. 4 was subjected to Flash-MPLC (silica gel; dichloromethane/ethyl acetate 99/1 to 100% ethyl acetate, then washed with 100% methanol) to afford 13 fractions (Fr. 4-1–4-13), Fr. 4-10 was subjected to MPLC (RP-C18 gel, H_2O/acetone 1/6, column size: 1.5 × 30 cm) to give 15 fractions (Fr. 4-10-1–4-10-13), Fr. 4-10-2 was subjected to MPLC (silica gel, *n*-hexane/acetone 3/1, column size: 1.5 × 30 cm) to produce 9 fractions (Fr. 4-10-2-1–4-10-2-9), Fr. 4-10-2-6 was subjected to an HPLC column (RP-C18, H_2O/acetonitrile 1 : 4) to obtain compound 7 (3.33 mg) and compound **8** (0.91 mg). Fr. 6 was subjected to MPLC (silica gel, *n*-hexane/acetone 3/1, column size: 2.5 × 25 cm) to afford 16 fractions (Fr. 6-1–6-16). Fr.6-8 was subjected to MPLC (silica gel, dichloromethane/acetone 10/1, column size: 1.5 × 30 cm) to give 16 fractions (Fr. 6-8-1–6-8-16), Fr.6-8-14 was subjected to an HPLC column (RP-C18, H_2O/acetonitrile 1 : 1) to obtain compound **5** (2.19 mg). Fr.6-11 was subjected to MPLC (silica gel, dichloromethane/acetone 5/1, column size: 1.0 × 30 cm) to give 12 fractions (Fr. 6-11-1–6-11-12). Fr. 6-11-11 was subjected to MPLC (RP-C18, H_2O/methanol 1/2, column size: 1.0 × 30 cm) to obtain compound **6** (2.70 mg). Fr. 10 was subjected to column chromatography (LH-20, methanol) to afford 12 fractions (Fr.10-1–10-12). Fr. 10-3 was subjected to MPLC (silica gel, dichloromethane/methanol 6/1, column size: 2.5 × 25 cm) to give 10 fractions (Fr. 10-3-1–10-3-10). Fr. 10-3-6 was subjected to MPLC (RP-C18, H_2O/acetone 4 : 7, column size: 1.5 × 30 cm) to produce 12 fractions (Fr. 10-3-6-1–10-3-6-12). Fr. 10-3-6-6 subjected to MPLC (silica gel, *n*-hexane/acetone 2/3, column size: 1.0 × 30 cm) to yield 6 fractions (Fr. 10-3-6-6-1–10-3-6-6-6). Fr. 10-3-6-6-3 was separated with prep. TLC (H_2O/acetone 1 : 1) to obtain compound **1** (1.45 mg) and compound **4** (5.01 mg). Fr. 10-3-6-9 subjected to MPLC (RP-C18, H_2O/acetone 1 : 2, column size: 1.0 × 30 cm) to obtain compound **2** (9.57 mg) and compound **3** (7.89 mg). The isolation flowchart of compounds **1–21** can be retrieved from the SI (Fig. S1).

Spectral data of previously undescribed compounds

Atriplexosaponin A (**1**): yellowish amorphous solid; IR (ATR) ν_{max}: 3375 (–OH), 1643 (C=C) cm^{-1}; ^1H NMR (CD_3OD, 800 MHz) and ^{13}C NMR data (CD_3OD, 200 MHz): see Table 1; HRESIMS $[M + Na]^+$ at *m*/*z* 835.4816 (calcd 835.4814 for $C_{43}H_{72}O_{14}Na^+$).

Atriplexosaponin B (**2**): yellowish amorphous solid; IR (ATR) ν_{max}: 3342 (–OH), 1644 (C=C) cm^{-1}; ^1H NMR (CD_3OD, 800 MHz) and ^{13}C NMR data (CD_3OD, 200 MHz): see Table 1; HRESIMS $[M + Na]^+$ at *m*/*z* 877.5282 (calcd 877.5284 for $C_{46}H_{78}O_{14}Na^+$).

Atriplexosaponin C (**3**): yellowish amorphous solid; IR (ATR) ν_{max}: 3383 (–OH), 1734 (C=O), 1643 (C=C) cm^{-1}; ^1H NMR (CD_3OD, 800 MHz) and ^{13}C NMR data (CD_3OD, 200 MHz): see Table 1; HRESIMS $[M + Na]^+$ at *m*/*z* 919.5381 (calcd 919.5389 for $C_{48}H_{80}O_{15}Na^+$).

Atriplexosaponin D (**4**): yellowish amorphous solid; IR (ATR) ν_{max}: 3363 (–OH), 1716 (C=O), 1643 (C=C) cm^{-1}; ^1H NMR (CD_3OD, 600 MHz) and ^{13}C NMR data (CD_3OD, 150 MHz): see Table 1; HRESIMS $[M + H]^+$ at *m*/*z* 1040.6522 (calcd 1040.6516 for $C_{55}H_{94}NO_{17}^+$).

Atriplexoterpene A (**5**): yellowish amorphous solid; IR (ATR) ν_{max}: 3394 (–OH), 1698 (C=O), 1652 (C=C) cm^{-1}; ^1H NMR (CD_3OD, 800 MHz) and ^{13}C NMR data (CD_3OD, 200 MHz): see Table 1; HRESIMS $[M + H]^+$ at *m*/*z* 471.3477 (calcd 471.3469 for $C_{30}H_{47}O_4^+$).

Atriplexoterpene B (**6**): yellowish amorphous solid; IR (ATR) ν_{max}: 3355 (–OH), 1652 (C=C) cm^{-1}; ^1H NMR (CD_3OD, 800 MHz) and 13C NMR data (CD_3OD, 200 MHz): see Table 1; HRESIMS $[M + H]^+$ at *m*/*z* 489.3576 (calcd 489.3575 for $C_{30}H_{49}O_5^+$).

Atriplexophyll A (**7**): greenish amorphous solid; V λ_{max} (MeOH) (log ε): 457 (3.69), 586 (2.84), 635 (3.21) nm; IR (ATR) ν_{max}: 3356 (–OH, –NH), 1705 (C=O), 1643 (C=C) cm^{-1}; ^1H NMR (CD_3OD, 600 MHz) and ^{13}C NMR data (CD_3OD, 150 MHz): see Table 2; HRESIMS $[M + H]^+$ at *m*/*z* 667.2770 (calcd 667.2762 for $C_{37}H_{39}N_4O_8^+$).

Atriplexophyll B (**8**): greenish amorphous solid; UV λ_{max} (MeOH) (log ε): 456 (3.63), 584 (2.70), 635 (3.06) nm; IR (ATR) ν_{max}: 3363 (–OH, –NH), 1705 (C=O), 1639 (C=C) cm^{-1}; ^1H NMR (CD_3OD, 600 MHz) and ^{13}C NMR data (CD_3OD, 200 MHz): see Table 2; HRESIMS $[M + H]^+$ at *m*/*z* 667.2768 (calcd 667.2762 for $C_{37}H_{39}N_4O_8^+$).

The phytochemical spectra of compounds **1–8** were accessible in the Supplementary Information (Fig. S2–S65).

Cell culture

HCT-116 (RRID: CVCL_0291), IEC-6 (RRID: CVCL_0343), and 3T3-L1 (RRID: CVCL_0123) cells were obtained from Bioresource Collection and Research Center (Hsinchu, Taiwan). HT-29 (RRID: CVCL_0320) cells were obtained from American Type Cell Collection (Manassas, VA, USA). HCT-116 and HT-29 cells were maintained in RPMI-1640 medium supplemented with 10% fetal bovine serum and 1× Antibiotic-Antimycotic at 37 °C in a humidified incubator with 5% CO_2. IEC-6 cells were cultured in DMEM media supplemented with 5% fetal bovine

Table 1 ^{1}H NMR and ^{13}C NMR data of compounds **1–4** in CD_3OD

Position		**1**		**2**		**3**		**4**	
		δ_H, mult (J in Hz) [a]	δ_C [c]	δ_H, mult[a] (J in Hz)	δ_C [c]	δ_H, mult[a] (J in Hz)	δ_C [c]	δ_H, mult[b] (J in Hz)	δ_C [d]
1	α	1.86, m	41.1	1.90, m	41.1	1.90, m	41.2	1.91, m	41.2
	β	1.26, m		1.27, m		1.27, m		1.28, m	
2	α	1.74, m	27.3	1.74, m	27.3	1.73, m	27.3	1.73, m	27.3
	β	1.95, m		1.94, m		1.94, m		1.94, m	
3	α	3.20, m	91.2	3.21, m	91.3	3.21, m	91.3	3.21, m	91.2
4		—	40.7	—	40.7	—	40.7	—	40.7
5	α	0.84, dd (12.0,1.6)	57.0	0.83, dd (12.0, 0.8)	57.0	0.82, d (12.0)	57.0	0.84, t (10.8)	57.0
6	α	1.46, m	19.4	1.45, m	19.4	1.44, m	19.3	1.45, m	19.3
	β	1.63, m		1.63, m		1.62, m		1.63, m	
7	α	1.57, m	34.3	1.56, m	34.4	1.55, m	34.4	1.56, m	34.4
	β	1.34, m		1.34, m		1.31, m		1.33, m	
8		—	41.6	—	41.6	—	41.7	—	44.45
9	α	1.68, d (8.4)	52.8	1.70, d (8.8)	53.0	1.69, d (8.8)	53.0	1.70, d (9.0)	53.1
10		—	39.0	—	39.0	—	39.0	—	39.0
11	β	3.86, dd (8.4, 2.8)	77.5	3.90, dd (8.8, 3.2)	76.0	3.89, dd (8.8, 3.2)	76.0	3.90, dd (9.6, 3.6)	76.0
12		5.44, d (2.8)	123.1	5.42, d (3.2)	124.0	5.42, d (3.2)	124.5	5.48, d (3.6)	124.9
13		—	149.0	—	148.3	—	147.9	—	146.9
14		—	44.46	—	44.57	—	44.4	—	44.52
15	α	1.39, m	36.6	1.39, m	36.6	1.34, m	36.1	1.37, m	36.5
	β	1.74, m		1.74, m		1.65, m		1.70, m	
16	α	4.27, dd (12.0, 4.8)	67.2	4.27, dd (12.0, 4.8)	67.3	4.29, dd (11.6, 5.2)	65.2	4.26, dd (11.7, 5.1)	67.5
17		—	44.64	—	44.59	—	44.6	—	44.6
18	β	2.31, dd (13.6, 4.8)	44.58	2.29, dd (14.4, 4.8)	44.5	2.53, dd (13.6, 4.8)	43.9	2.49, dd (13.8, 4.8)	43.1
19	α	1.73, m	47.6	1.71, m	47.6	1.75, m	47.4	1.90, m	47.7
	β	1.12, m		1.12, m		1.14, m		1.27, m	
20		—	31.7	—	31.7	—	31.6	—	36.3
21	α	1.45, m	34.7	1.45, m	34.7	1.47, m	34.7		77.3
	β	1.24, m		1.23, m		1.22, m		4.93, dd (12.0, 4.8)	
22	α	1.48, m	25.7	1.47, m	25.7	1.61, m	24.1	1.59, m	30.0
	β	2.11, m		2.11, m		1.82, m		2.20, m	
23	β	0.89, s	16.9	0.89, s	16.9	0.89, s	16.9	0.88, s	16.9
24	α	1.10, s	28.5	1.10, s	28.5	1.10, s	28.5	1.10, s	28.5
25	β	1.09, s	17.6	1.08, s	17.6	1.08, s	17.6	1.085, s	17.6
26	β	1.06, s	18.7	1.06, s	18.7	1.04, s	18.8	1.04, s	18.8
27	α	1.31, s	26.5	1.31, s	26.4	1.32, s	26.6	1.31, s	26.3
28	β	3.29, d (10.8)	68.4	3.29, d (11.2)	68.4	3.97, d (11.2)	67.548	3.35, d (11.2)	66.3
		3.77, d (10.8)		3.77, d (11.2)		4.06, d (11.2)		3.63, d (11.2)	
29	β	0.96, s	24.2	0.95, s	24.2	0.97, s	24.07	1.01, s	18.7
30	α	0.92, s	33.6	0.92, s	33.6	0.92, s	33.5	0.89, s	29.3
1′	α	4.44, d (8.3)	105.4	4.45, d (8.1)	105.4	4.45, d (8.2)	105.4	4.45, d (8.0)	105.4
2′	β	3.57, t (8.3)	81.1	3.58, t (8.1)	81.1	3.58, t (8.2)	81.0	3.58, t (8.0)	81.1
3′	α	3.55, t (8.3)	78.5	3.56, t (8.1)	78.5	3.56, t (8.2)	78.5	3.56, t (8.0)	78.6
4′	β	3.29, t (8.3)	71.6	3.29, t (8.1)	71.6	3.30, t (8.2)	71.6	3.30, t (8.0)	71.6
5′	α	3.27, m	77.7	3.27, m	77.6	3.27, m	77.6	3.28, m	77.6
6′	β	3.66, dd (12.0, 5.6)	62.8	3.66, dd (12.0, 5.6)	62.8	3.66, dd (12.0, 5.6)	62.8	3.62, dd (11.9, 5.4)	62.8
		3.86, dd (12.0, 1.6)		3.85, dd (12.0, 1.6)		3.85, dd (12.0, 2.4)		3.85, dd (11.9, 2.1)	
1″	α	4.68, d (8.0)	104.5	4.68, d (8.8)	104.5	4.68, d (8.7)	104.5	4.68, d (8.7)	104.5
2″	β	3.23, dd (8.0, 8.9)	76.3	3.22, t (8.8)	76.3	3.22, t (8.7)	76.3	3.23, t (8.7)	76.3
3″	α	3.36, t (8.9)	77.9	3.36, t (8.8)	77.9	3.36, t (8.7)	77.9	3.36, t (8.7)	77.9
4″	β	3.20, t (8.9)	71.9	3.20, t (8.8)	72.0	3.20, t (8.7)	72.0	3.22, t (8.7)	72.0
5″	α	3.26, m	78.4	3.25, m	78.4	3.25, m	78.4	3.25, m	78.4
6″	β	3.62, dd (12.0, 6.4)	63.1	3.62, dd (12.0, 6.4)	63.2	3.61, dd (12.0, 6.4)	63.2	3.67, dd (12.0, 5.4)	63.2
		3.83, dd (12.0, 1.6)		3.83, dd (12.0, 1.6)		3.83, dd (12.0, 2.4)		3.83, dd (12.0, 2.4)	
1‴		3.24, s (OCH_3)	54.5	3.30, m/3.52, m	67.4	3.31, m/3.53, m	67.549	3.31, m/3.53, m	67.6
2‴				1.47, m	33.6	1.48, m	33.6	1.47, m	33.6
3‴				1.35, m	20.5	1.36, m	20.5	1.37, m	20.5
4‴				0.92, t (7.2)	14.3	0.92, t (7.6)	14.3	0.92, t (7.5)	14.3
1⁗						—	173.1	—	179.6
2⁗						2.06, s	20.9	2.21, m	43.9
3⁗								1.41, m/1.60, m	28.3
4⁗								0.89, t (7.5)	12.3

Table 1 (*Contd.*)

	1		2		3		4	
Position	δ_H, mult (J in Hz) [a]	δ_C [c]	δ_H, mult[a] (J in Hz)	δ_C [c]	δ_H, mult[a] (J in Hz)	δ_C [c]	δ_H, mult[b] (J in Hz)	δ_C [d]
5‴′							1.09, d (7.2)	18.1
1‴″							—	174.7
2‴″							2.38, m	32.8
3‴″							1.82, m	26.1
4‴″							3.22, m	39.5

[a] ^{1}H NMR data measured at 800 MHz. [b] ^{1}H NMR data measured at 600 MHz. [c] ^{13}C NMR data measured at 200 MHz. [d] ^{13}C NMR data measured at 150 MHz.

Table 2 ^{1}H NMR and ^{13}C NMR data of compounds **5** and **6** in CD_3OD

		5		6	
Position		δ_H, mult[a] (J in Hz)	δ_C [b]	δ_H, mult[a] (J in Hz)	δ_C [b]
1	α	2.10, m	40.0	1.85, m	39.2
	β	1.44, m		0.95, m	
2	α	2.43, m	34.8	1.66, m	27.3
	β	2.62, m		1.70, m	
3		—	219.9	α 3.61, dd (11.2, 4.8)	73.4
4		—	49.7	—	43.5
5	α	1.42, dd (12.4, 2.8)	55.6	1.15, m	48.4
6	α	1.56, m	19.9	1.53, m	18.4
	β	1.71, m		1.54, m	
7	α	1.51, m	31.8	1.56, m	32.1
	β	1.30, m		1.22, m	
8		—	42.8	—	43.1
9	α	1.99, brs	53.1	1.91, brs	54.0
10		—	37.2	—	37.2
11		5.95, dd (10.4, 2.4)	133.7	5.96, dd (10.4, 2.4)	134.4
12		5.42, dd (10.4, 2.4)	130.9	5.39, dd (10.4, 2.4)	130.3
13		—	85.2	—	85.6
14		—	46.4	—	45.7
15	α	1.46, dd (12.2, 6.0)	36.1	1.44, m	36.1
	β	1.61, dd (12.2, 10.2)		1.64, m	
16	α	4.12, dd (10.2, 6.0)	66.5	4.61, dd (9.6, 5.6)	67.7
17		—	37.4	—	50.1
18	β	1.82, m	52.3	1.77, m	52.7
19	α	1.82, m	38.0	1.76, m	37.6
	β	1.36, m		1.22, m	
20		—	35.8	—	34.2
21	α		74.2	1.64, m	45.2
	β	3.58, dd (12.0, 4.0)		1.55, m	
22	α	1.22, m	34.2		76.5
	β	2.26, m		3.87, dd (12.0, 4.8)	
23	β	1.05, s	21.2	0.69, s	12.1
24	α	1.08, s	26.6	3.30, d (10.4)	66.7
				3.53, d (10.4)	
25	β	1.04, s	17.7	0.95, s	25.0
26	β	1.13, s	19.6	1.11, s	33.6
27	α	1.030, s	20.8	1.05, s	21.4
28	β	3.10, d (7.2)	72.9	3.33, d (7.2)	72.8
		3.90, d (7.2)		4.25, d (7.2)	
29	β	0.88, s	17.8	0.96, s	25.0
30	α	1.026, s	30.2	1.04, s	33.6

[a] ^{1}H NMR data measured at 800 MHz. [b] ^{13}C NMR data measured at 200 MHz.

serum, 1× Antibiotic-Antimycotic, and 0.1 unit mL^{-1} insulin. 3T3-L1 cells were cultured in DMEM media supplemented with 10% fetal bovine serum and 1× Antibiotic-Antimycotic.

Cell viability

Cells were treated with DMSO or the indicated compounds, followed by incubation with the Enhanced Cell Counting Kit 8 (WST-8/CCK8; Cat# E-CK-A362, Elabscience, Houston, TX, USA) at 37 °C. Cell viability was then assessed spectrophotometrically at 450 nm (n = 3 in each group). Statistical analysis was performed using GraphPad Prism software (GraphPad, San Diego, CA, USA). Differences between groups were analyzed by Student's t-test, and p-values <0.05 were considered statistically significant.

Results and discussion

In the current study, we applied an FBMN-guided approach to investigate the chemical composition of *A. maximowicziana* (Fig. 1). Our goal was to identify previously uncharacterized constituents and evaluate their potential anticancer activities, particularly against colorectal cancer (CRC), a malignancy with rising incidence and urgent therapeutic needs. This study led to the isolation and structural elucidation of eight previously undescribed metabolites, comprising atriplexosaponins A–D (**1–4**, triterpenoid saponins), atriplexoterpenes A–B (**5–6**, triterpenoids), and atriplexophylls A–B (**7–8**, chlorophyll derivatives), along with thirteen known compounds (**9–21**) from the *n*-hexane layer and *n*-butanol layer of *A. maximowicziana* (See Fig. 4 and SI: Fig. S1). In addition, 18 isolates (**1–17**, **19**) with sufficient amounts were further examined for the effects on cell viability in HT-29 and HCT-116 cancer cell lines.

FBMN of *A. maximowicziana*

A total of eleven fractions derived from the *n*-hexane and *n*-butanol layers of *A. maximowicziana* methanolic extract were analyzed using GNPS platform to generate a visualizable FBMN (Fig. 1). After compound classification with the NP Classifier by SIRUS, tryptophan alkaloids and triterpenoids have been found as the two most predominant structure classes among 62 NP Classifier superclasses, accounting for 14% and 13% of the total

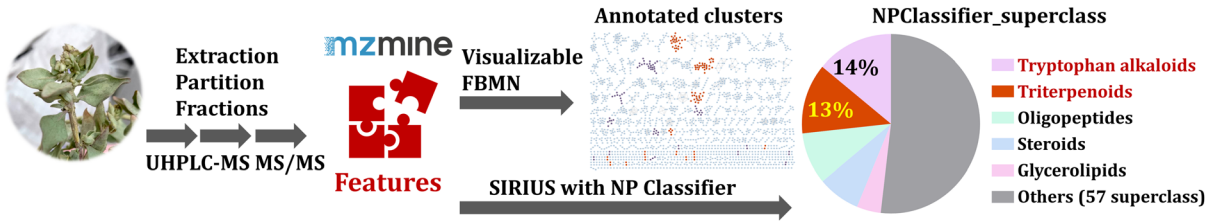

Fig. 1 Feature-based molecular networking (FBMN) and feature classes of *A. maximowicziana*. Features from fractions of *A. maximowicziana* by the software mzmine to generate a visualizable FBMN on the GNPS platform and to calculate feature classes by NP Classifier in the software SIRIUS. The intensity of NPClassifier_superclass with features presented as a pie chart. The clusters described in this paper were annotated on the visible FBMN thumbnail.

NPClassifier_superclass intensity, respectively (Fig. 1). Triterpenoids were selected as the primary target for further investigation due to the structural consistency of their core skeleton. The triterpenoid clusters of FBMN picture were assigned based on the intensity of NPClassifier_superclass triterpenoids exceeding 70 percent in each cluster, and were distinguished as triterpenoids molecular family and triterpenoid-saponins molecular family by the absence or presence of sugar units in their structure (Fig. 2a). Subsequent analysis of the intensity among fractions revealed that fractions 6, 7, 9, and 10 were enriched in triterpenoids (Fig. 2b), while fractions 7, 9, and 10 were particularly abundant in triterpenoid saponins (Fig. 2c). Fraction 6 was selected for the isolation of triterpenoids because of its unique distinct enrichment, whereas fraction 10 was prioritized for the purification of triterpenoid saponins based on its dominant intensity. The isolated compounds (Fig. 4) and the triterpenoid node annotated by the GNPS library are shown in the FBMN picture (Fig. 2a), proving the beneficial effects of the separation approach.

Tryptophan alkaloids refer to a diverse group of compounds with various skeletons. To enable a more detailed evaluation of tryptophan alkaloids, these features were classified using

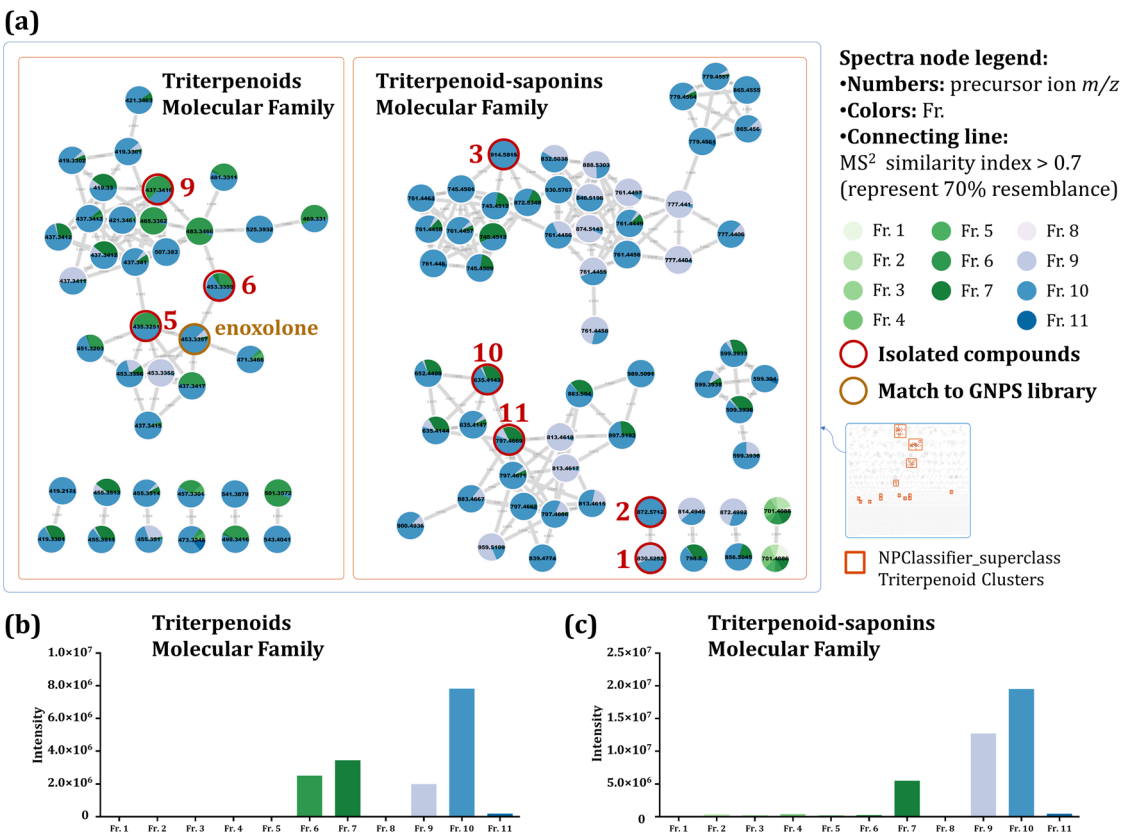

Fig. 2 Feature-based molecular networking (FBMN) of triterpenoids in *A. maximowicziana*. (a) Painted by the fractions of *n*-hexane and *n*-butanol layers from *A. maximowicziana* methanolic extract. NPClassifier_superclass triterpenoids clusters (triterpenoids molecular family and triterpenoid-saponins molecular family) in the orange rectangles, isolated compounds in the red circles, and nodes matched the GNPS library in brown circles. (b) Triterpenoids molecular family intensity from fractions. (c) Triterpenoid-saponins molecular family intensity from fractions.

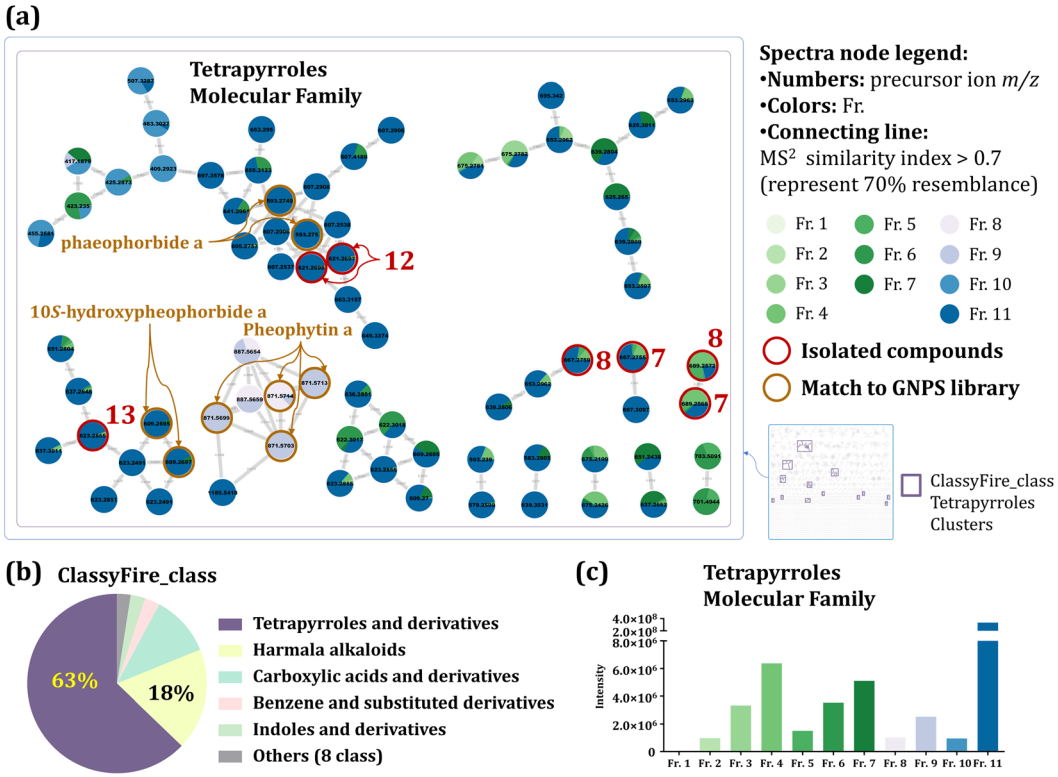

Fig. 3 Feature-based molecular networking (FBMN) of tetrapyrroles in *A. maximowicziana*. (a) Painted by the fractions of *n*-hexane and *n*-butanol layers from *A. maximowicziana* methanolic extract. ClassyFire_class tetrapyrroles clusters (tetrapyrroles molecular family) in the purple rectangles, isolated compounds in the red circles, and nodes matched the GNPS library in brown circles. (b) The intensity of ClassyFire_class inside NPClassifier_superclass Tryptophan alkaloids. (c) Tetrapyrroles molecular family intensity from fractions.

ClassyFire through the SIRIUS platform. After that, the ClassyFire_class "Tetrapyrroles and derivatives" has been found as the predominant compound structures of NPClassifier_superclass tryptophan alkaloids, offering 63% intensity (Fig. 3b). Tetrapyrroles have been selected as the secondary target for investigation. Molecular family clusters corresponding to tetrapyrroles were identified in the FBMN map based on two criteria: clusters in which the ClassyFire classification "Tetrapyrroles and derivatives" accounted for more than 70% of the node intensity, and the presence of nodes matched to tetrapyrrole reference spectra in the GNPS library (Fig. 3a). Further analysis of molecular family intensity among fractions revealed that fractions 4 and 11 were the most enriched in tetrapyrroles (Fig. 3c) and were therefore selected for targeted isolation. The isolated compounds and the tetrapyrrole nodes identified by the GNPS library are also depicted in the FBMN picture (Fig. 2a).

Triterpenoids and tetrapyrroles were delineated as the predominant structural classes in *A. maximowicziana* based on the FBMN workflow on GNPS and SIRIUS. To validate these assignments, reveal structurally unprecedented metabolites, and pinpoint candidates for further pharmacological investigation, fractions enriched in these two families were subjected to targeted purification. The ensuing section details the structural elucidation of previously undescribed compounds and subsequent evaluation of the anticancer activity of sufficient compounds, laying the groundwork for structure–activity relationship analysis.

Structure elucidation

Compound **1** was obtained as a yellowish amorphous solid. Its molecular formula was determined to be $C_{43}H_{72}O_{14}$ from HRESIMS ($[M + Na]^+$ at *m/z* 835.4816 (calcd 835.4814 for $C_{43}H_{72}O_{14}Na^+$)), implying eight degrees of unsaturation. The hydroxy (3375 cm^{-1}) group and C=C unit (1643 cm^{-1}) were observed in the IR spectrum. The ^1H NMR spectrum (Table 1) displayed signals of seven singlet methyl groups at δ_H 0.89 (3H, s, H-23), 0.92 (3H, s, H-30), 0.96 (3H, s, H-29), 1.06 (3H, s, H-26), 1.09 (3H, s, H-25), 1.10 (3H, s, H-24), and 1.31 (3H, s, H-27), one methoxy at δ_H 3.24 (3H, s, OCH_3), and one trisubstituted olefinic proton at δ_H 5.44 (1H, d, J = 2.8 Hz, H-12). Two anomeric proton signals at δ_H 4.44 (1H, d, J = 8.3 Hz, H-1′) and 4.68 (1H, d, J = 8.0 Hz, H-1″) indicated the presence of two sugar moieties. The ^{13}C NMR (Table 1) and DEPT spectra showed forty-three resonances comprising eight methyls, eleven methylenes, seventeen methines, and seven quaternary carbons. Based on the HMBC correlation (Fig. 5) between H_3-29/C-19, C-20, C-21, C-30, H_3-30/C-19, C-20, C-21, C-29 indicated that the dimethyl group at C-20. The above information suggested compound **1** was a triterpenoidal saponin, reminiscent of an olean-12-ene pentacyclic triterpenoid framework with two sugar units. The aglycon framework spectroscopic data of **1** (Table 1) is comparable with those of the literature compound β-amyrin,[31] except for a methoxy group at C-11, a hydroxy group at C-16, and a hydroxymethyl group at C-17 in compound **1**. Based

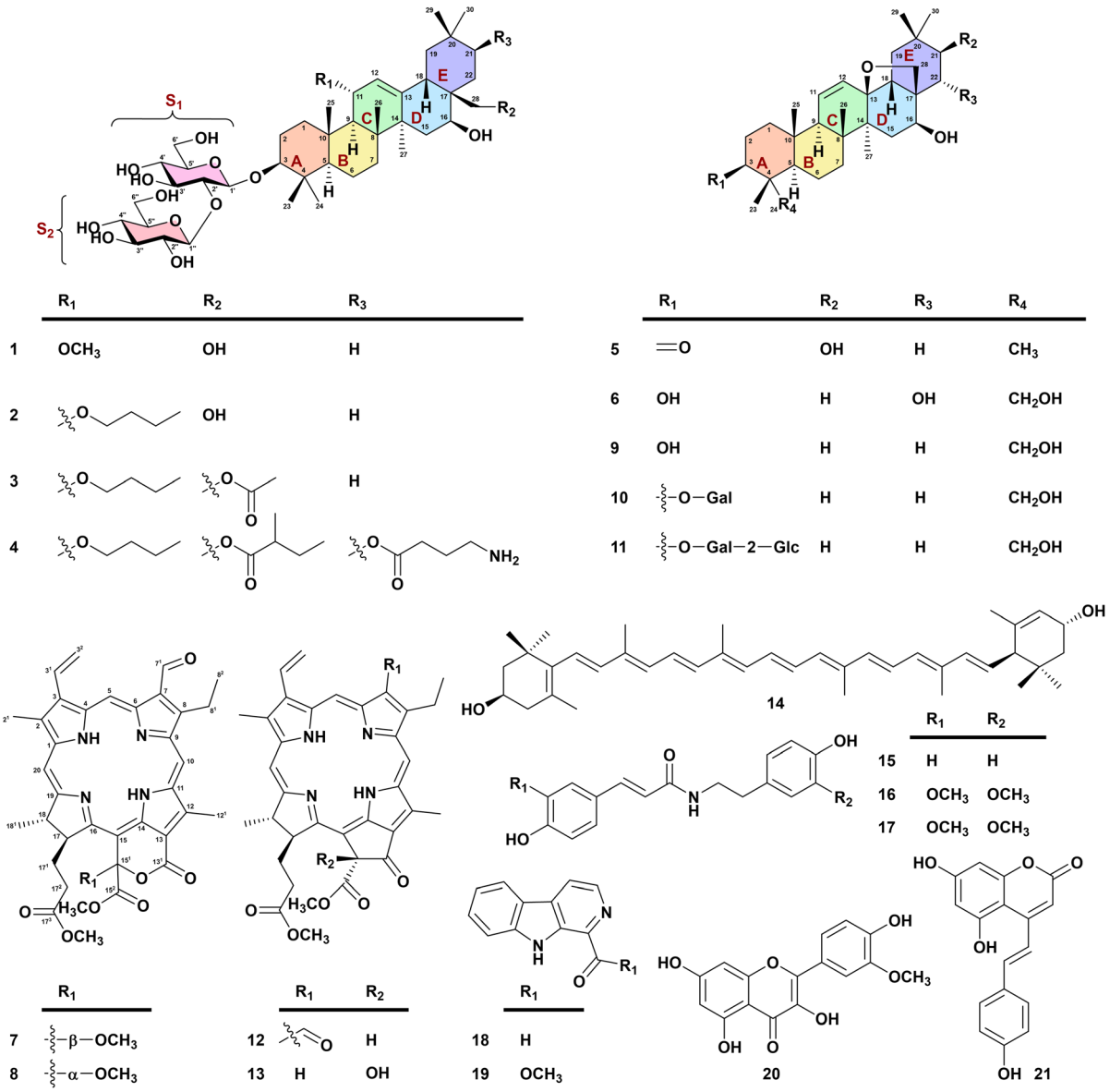

Fig. 4 Structures of compounds **1**–**21**.

on the HMBC correlation between OCH_3-11/C-11, the methoxy group (OCH_3-11) was at C-11. The downfield shift of H-16 (δ_H 4.27 (1H, dd, J = 12.0, 4.8 Hz)) and the COSY correlation (Fig. 5) of H-15/H-16 implied that the hydroxy group was connected with C-16. The hydroxymethyl group was at C-17 from HMBC correlations of H_2-28/C-16, C-17, C-22. The NOESY correlation (Fig. 6) between H-3/H-5, H-5/H-9, H-9/H_3-27, H_3-27/H-16, and H_2-19 indicated H-3, H-5, H-9, H-16, and H_3-27 all adopt an α-axial orientation, while the D and E rings are *cis*-fused. In the NOESY spectra, the correlations of H_3-23/H_3-25, H_3-25/H-11, H-11/H_3-26, H_3-26/H-15β, and H-15β/H_2-28 indicated that H-11, H-15β, H_3-23, H_3-25, H_3-26, and H_2-28 were in β-axial position. The NOESY plot of H-19α/H_3-30 and the absence of H-19α/H_3-29 also suggested H-19α in the α-axial position, H_3-29 in the β-axial, and H_3-30 in the α-equatorial configuration of ring E.

The two sugar moieties of **1** were determined to be glucopyranose based on the remaining ten oxymethines and two oxymethylenes from ^{1}H and ^{13}C NMR spectra. The coupling constants of the anomeric proton signals of both sugar moieties, J = 8.3 of H-1′ and J = 8.0 Hz of H-1″ agree with their β-configuration. The 1D-selective TOCSY experiment was performed to resolve the overlapping proton signals of sugar moieties using a 20 msec mixing time (Fig. 7). The large coupling constant (J > 8Hz)[32] of H-1′–H-4′, H-1″–H-4″, and the NOESY correlation between H-1′/H-3′, H-5′, H-2′/H-6′, and H-1″/H-3″, H-5″ pointed that two sugar moieties (S_1 and S_2) are typical glucoses. The connectivity between triterpenoid and two glucose units were established through HMBC correlation between H-1′/H-3 and H-1″/H-2′. Based on the above evidence, the structure of **1** was identified and named atriplexosaponin A.

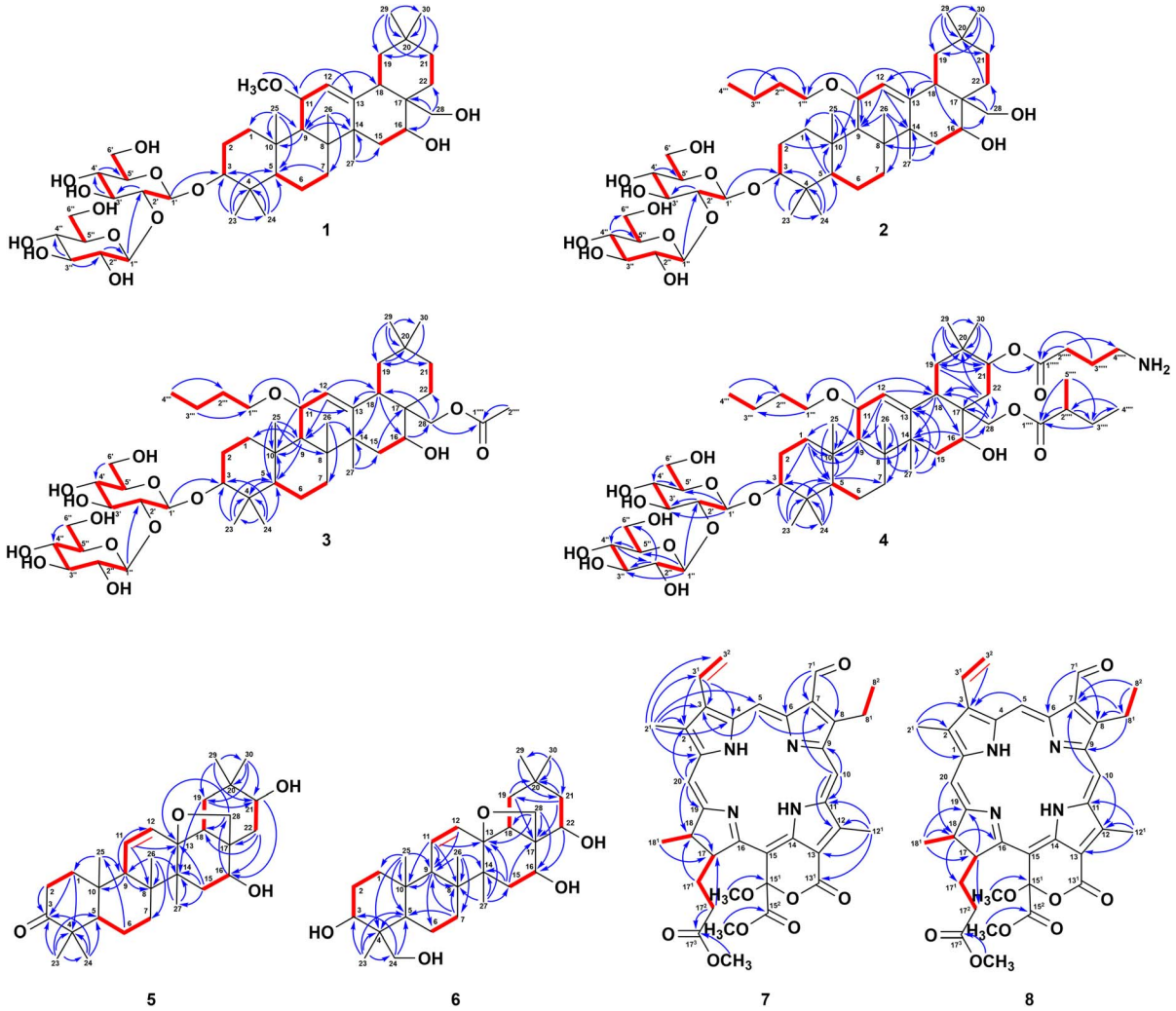

Fig. 5 Key $^{1}H-^{1}H$ COSY (—) and HMBC (H→C) correlations of **1**–**8**.

Compound **2** was isolated as a yellowish amorphous solid, and the molecular formula was determined to be $C_{46}H_{78}O_{14}$ from HRESIMS ($[M + Na]^+$ at *m*/*z* 877.5282 (calcd 877.5284 for $C_{46}H_{78}O_{14}Na^+$)), implying eight degrees of unsaturation. The hydroxy (3342 cm^{-1}) group and C=C unit (1644 cm^{-1}) were observed in the IR spectrum. The physical data and NMR spectroscopic data of **2** and **1** (Table 1) implied their similar structure, except that the methoxy group (OCH_3-11) in **1** was changed to an *n*-butoxy group in **2**. The COSY correlation (Fig. 5) of H_3-4‴/H_2-3‴, H_2-3‴/H_2-2‴, H_2-2‴/H_2-1‴, and the HMBC plots (Fig. 5) of H_3-4‴/C-2‴, H_2-3‴/C-1‴, H-11/C-1‴ verified that a *n*-butoxy group were attached to C-11. As the same NOESY correlations (Fig. 6) as those of **1**, the relative configurations of **2** were assigned, and the *n*-butoxy group was at the β-equatorial face. As determined by the above observations, compound **2** was elucidated and named atriplexosaponin B.

Compound **3**, a yellowish amorphous solid, was established with its molecular formula as $C_{48}H_{80}O_{15}$ based on HRESIMS ($[M + Na]^+$ at *m*/*z* 919.5381 (calcd 919.5389 for $C_{48}H_{80}O_{15}Na^+$)), implying nine degrees of unsaturation. The IR and NMR spectra data of **3** were similar to those of **2**, except for an additional acetoxy group signal in **3** (IR ν_{max}: 1734 cm^{-1}; δ_H 2.06, s (H-2‴′); δ_C 173.1 (C-1‴′). The HMBC correlation (Fig. 5) of H_2-28/C-1‴′, H_3-2‴′/C-1‴′ verified that an acetoxy group was attached to C-28 to form an acetoxymethyl group at C-17. Due to the similar NOESY correlation to **1** (Fig. 6), the relative configurations of **3** were determined, and the acetoxymethyl group was at the α-axial position. Therefore, the structure of **3** was defined and named atriplexosaponin C.

Compound **4** was obtained as a yellowish amorphous solid. Its molecular formula was determined to be $C_{55}H_{93}NO_{17}$ from HRESIMS ($[M + H]^+$ at *m*/*z* 1040.6522 (calcd 1040.6516 for $C_{55}H_{94}NO_{17}^+$)), implying ten degrees of unsaturation. The IR and NMR spectroscopic data of **4** were similar to those of **3** (Table 1), except for the substituent difference of C-21 (**3**: hydrogen; **4**: 4-aminobutanoylmethyl group) and C-28 (**3**: acetoxy group; **4**: 2-2-methylbutanoyloxyl group). The COSY correlation (Fig. 5) of H_2-2⁗′/H_2-3⁗′, H_2-3⁗′/H_2-4⁗′ and the HMBC (Fig. 5) correlation of H_2-2⁗′/C-1⁗′, H_2-3⁗′/C-1⁗′, H_2-2⁗′/C-4⁗′ verified the existence of a 4-aminobutanoate group, and the

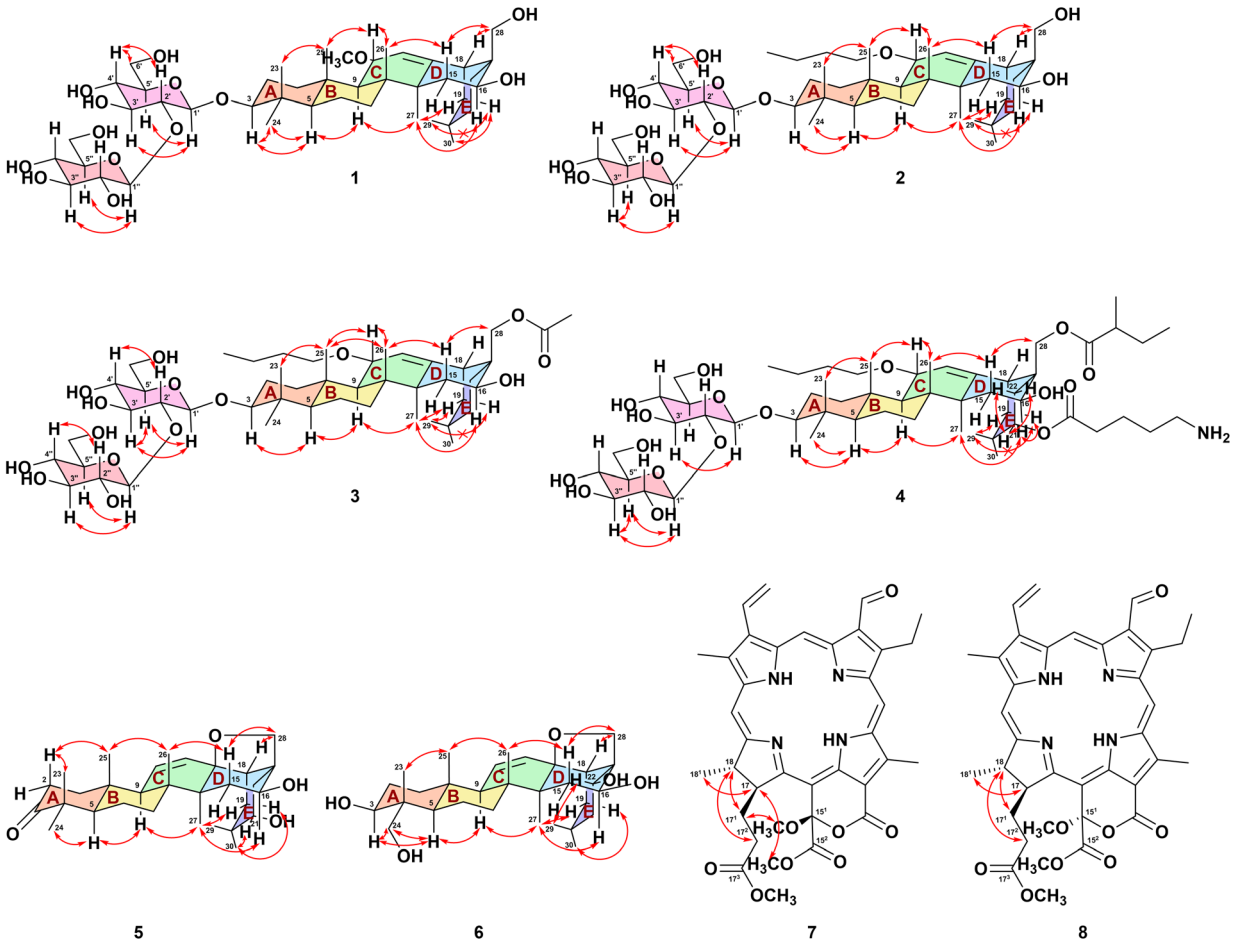

Fig. 6 Key $^{1}H-^{1}H$ NOESY (↔) correlations of **1**–**8**.

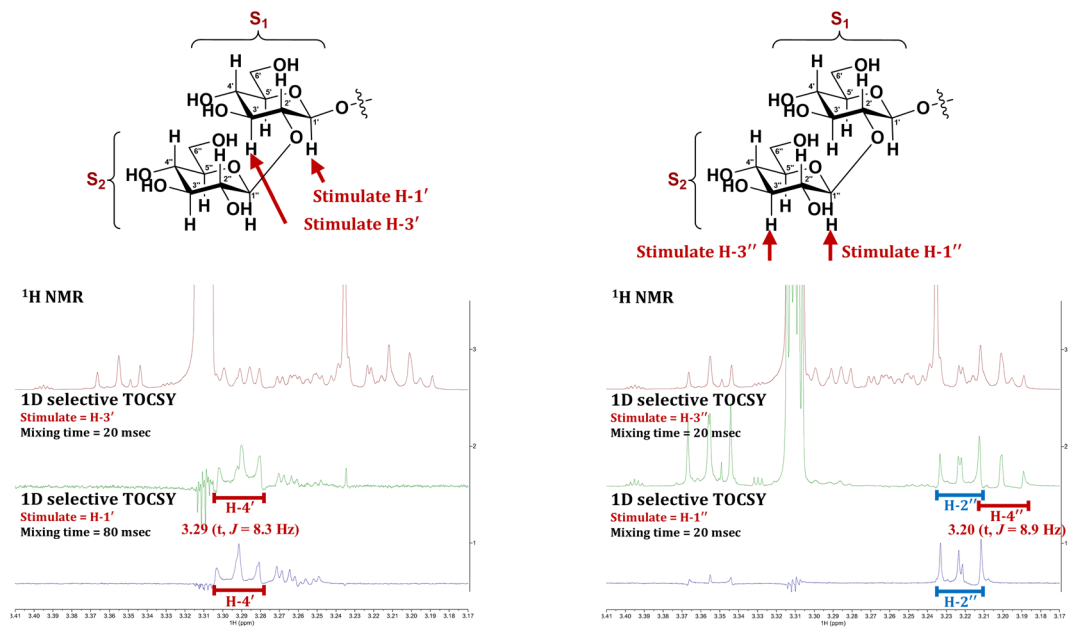

Fig. 7 1D-selective TOCSY spectra of **1**.

HMBC plot of H-21/C-1′′′′′ indicated that the 4-aminobutanoylmethyl group was attached on C-21. Further analysis of the HMBC correlations between H-2′′′′/C-1′′′′, H-2′′′′/C-3′′′′, H_2-3′′′′/C-1′′′′, H_2-3′′′′/C-4′′′′, H_3-4′′′′/C-2′′′′, H_3-5′′′′/C-1′′′′, H_3-5′′′′/C-3′′′′ verified that the acetoxy group at C-28 in compound **3** was replaced by the 2-methylbutanoyloxyl group in compound **4**. Based on the similarity of the NOESY correlations compared to those of **3** (Fig. 6), the relative configuration of **4** was established, confirming that both the 4-aminobutanoylmethyl and 2-methylbutanoyloxymethyl groups are oriented in β-axial positions. Thus, the structure of compound **4** was assigned and named atriplexosaponin D.

Compound **5** was obtained as a yellowish amorphous solid. Its molecular formula was determined to be $C_{30}H_{46}O_4$ from HRESIMS ($[M + H]^+$ at *m*/*z* 471.3477 (calcd 471.3469 for $C_{30}H_{47}O_4^+$)), implying eight degrees of unsaturation. The hydroxy (3394 cm^{-1}) group, C=O unit (1698 cm^{-1}), and C=C unit (1652 cm^{-1}) were observed in the IR spectrum. The physical data and NMR spectroscopic data of **5** (Table 2) are comparable with those of the literature compound 13,28-epoxy-olean-11-en-16-ol-3-one,[33] except for an additional hydroxy group at C-21 in **5**. The downfield shift of C-21 (Table 2) (**5**: δ_C 74.2 ppm), the COSY plot (Fig. 5) of H_2-22/H-21 and the HMBC correlation (Fig. 5) between H_2-19/C-21, H_3-29/C-21, H_3-30/C-21 demonstrated that a hydroxy group was attached to C-21. The NOESY correlation (Fig. 6) between H-5/H-9, H-9/H-27, H-27/H-16, H-19 verified H-5, H-9, CH_3-27, H-16 were in α-axial position whereas OH-16 occupies an β-equatorial position. Furthermore, the D and E rings are *cis*-fused. In the NOESY spectra, **5** revealed correlations between H-2_{ax}/H-23, H-25, H-25/H-26, H-26/H-15_{ax}, H-15_{ax}/H_2-28 indicated that H-2_{ax}, H-15_{ax}, CH_3-23, CH_3-25, CH_3-26, and H_2-28 were in β-axial position. As the same NMR-based empirical rules of **1** (Fig. 5), the relative configuration of ring E was defined, revealing that H-21 occupies the β-equatorial position, and CH_3-29 occupies the β-axial position. On the basis of the above rules, the structure of compound **5** was assigned and named atriplexoterpene A.

Compound **6** was obtained as a yellowish amorphous solid. Its molecular formula was determined to be $C_{30}H_{48}O_5$ from HRESIMS ($[M + H]^+$ at *m*/*z* 489.3576 (calcd 489.3575 for $C_{30}H_{49}O_5^+$)), implying seven degrees of unsaturation. Comparing the ^1H and ^{13}C NMR spectra of **6** to **5**, the downfield shift of H-24 (δ_H 3.30/3.53) indicated the methyl group in **5** (C-24) was oxygenated in **6**. Furthermore, the hydroxy group at C-21 in **5** was shifted to C-22 based on the downfield shift of H-22 (δ_H 3.87), the COSY correlation (Fig. 5) of H_2-21/H-22, and the HMBC correlation (Fig. 5) of H-22/C-16. Within the similar NOESY plots to those of **5** (Fig. 6), the relative configurations of H-3, H-22, and H-24 were in α-axial, β-axial, and α-equatorial positions, respectively. Therefore, the structure of compound **6** was established and named atriplexoterpene B.

Compounds **7** and **8** are HPLC-separable stereoisomers and share the same planar structure as 15^2-methoxy lactone pheophorbide-b methyl ester.[34] However, the literature only reported the planner structure of 15^2-methoxy lactone pheophorbide-b methyl ester with MS spectral data, lacking supportive NMR evidence.[34] In this study, we have successfully isolated these two stereoisomeric compounds for the first time and provided their UV, IR, and NMR spectral data. The structural elucidation of these two compounds will be discussed individually in the following sections.

Compound **7** was obtained as a greenish amorphous solid. Its molecular formula was determined to be $C_{37}H_{38}N_4O_8$ from HRESIMS ($[M + H]^+$ at *m*/*z* 667.2770 (calcd 667.2762 for $C_{37}H_{39}N_4O_8^+$)), implying twenty-one degrees of unsaturation. The hydroxy (3355 cm^{-1}) group, C=O unit (1705 cm^{-1}), and

Table 3 ^1H NMR and ^{13}C NMR data of compounds **7** and **8** in CD_3OD

		7		**8**	
Position		δ_H, mult (*J* in Hz) [a]	δ_C [b]	δ_H, mult (*J* in Hz) [a]	δ_C [c]
1		—	158.2	—	158.2
2		—	136.9	—	136.9
2^1		3.23, s	12.2	3.24, s	12.2
3		—	141.7	—	141.7
3^1		7.93, dd (17.9, 11.6)	131.2	7.95, dd (17.9, 14.4)	131.2
3^2		5.98, dd (11.6, 1.5) 6.23, dd (17.9, 1.5)	120.4	5.99, dd (14.4, 1.7) 6.24, dd (17.9, 1.7)	120.4
4		—	149.7	—	149.7
5		9.99, s	105.8	10.03, s	106.1
6		—	148.3	—	148.3
7		—	156.1	—	156.2
7^1		11.14, s	189.9	11.16, s	189.9
8		—	131.6	—	131.7
8^1		4.16, q (7.7)	20.0	4.18, q (7.6)	20.0
8^2		1.82, t (7.7)	19.8	1.84, t (7.6)	19.8
9		—	142.2	—	142.2
10		9.70, s	110.4	9.73, s	110.5
11		—	143.9	—	144.0
12		—	149.1	—	149.2
12^1		3.72, s	12.6	3.72, s	12.7
13		—	117.3	—	116.9
13^1		—	164.6	—	164.8
14		—	149.1	—	149.6
15		—	100.8	—	99.0
15^1		—	108.8	—	108.4
15^2		—	171.1	—	175.4
16		—	166.0	—	165.0
17	α	4.59, m	55.4	4.66, m	53.4
17^1	β	2.03, m/2.54, m	33.8	2.36, m/2.53, m	31.2
17^2		2.40, m/2.62, m	33.0	1.72, m/1.75, m	32.7
17^3		—	175.9	—	170.9
18	β	4.32, q (7.3)	49.9	4.29, q (7.2)	50.6
18^1	α	1.55, d (7.3)	23.3	1.69, d (7.2)	22.9
19		—	170.6	—	170.4
20		8.33, s	65.1	8.36, s	95.2
15^1-OCH_3	α		53.3	3.54, s	51.7
	β	3.89, s			
15^2-OCH_3		3.54, s	53.4	3.54, s	51.7
17^3-OCH_3		3.63, s	52.1	3.68, s	53.9

[a] ^1H NMR data measured at 600 MHz. [b] ^{13}C NMR data measured at 200 MHz. [c] ^{13}C NMR data measured at 150 MHz.

C=C unit (1652 cm^{-1}) were observed in the IR spectrum. The UV absorption at 457, 586, and 635 nm suggested 7 belong to chlorophyll-related compounds. The ^1H signals (Table 3) of three meso-olefinic protons at δ_H 8.33 (1H, s, H-20), 9.70 (1H, s, H-10), 9.99 (1H, s, H-5), and the vinyl group at δ_H 5.98 (1H, dd, J = 11.6, 1.5 Hz, H-3^2b), 6.23 (1H, dd, J = 17.9, 1.5 Hz, H-3^2a), 7.93 (1H, dd, J = 17.9, 11.6 Hz, H-3^1) indicated the presence of typical porphyrin. The proton signal of the aldehyde group at δ_H 11.14 (1H, s, H-7^1) stated that 7 belongs to chlorophyll-*b* type compounds. The COSY correlation (Fig. 5) of H-17/H_2-17^1, H_2-17^2/H_2-17^1 and the HMBC correlation (Fig. 5) of H-17^1/C-18, H-17^2/C-17, H-17^2/C-17^3, H_3-18^1/C-17, with the methoxy group δ_H 3.63 (1H, s, H-17^3-OCH_3)/C-17^3, indicated a methyl butyrate group on C-17. The carbon signals (Table 3) at δ_C 117.3 (C-13), δ_C 149.1 (C-14), δ_C 164.6 (C-13^1), δ_C 100.8 (C-15), δ_C 108.8 (C-15^1), and the HMBC correlation of H-12^1/C-13, H-12^1/C-13^1 verified that a pyran formed with three carbons C-13, C-14, C-15 of porphyrin, an ester group at C-13^1, and the carbon C-15. The carbon signals at δ_C 108.8 (C-15^1) and δ_C 171.1 (C-15^1–OCH_3) combine with the HMBC correlation of the methoxy group δ_H 3.89 (1H, s, H_3-15^1–OCH_3)/C-15^1 and the methoxy group δ_H 3.54 (1H, s, H-15^2–OCH_3)/C-15^2, verifying two methoxy groups on C-15^1 and C-15^2, respectively. The relative configuration of compound 7 was determined based on NOESY correlations (Fig. 6). Cross-peaks between H-17/H_3-18^1, H_2-17^1/H-18, and H_2-17^2/H-18 indicated that H_3-18^1 and H_2-17^1 are in opposite phases. Additionally, NOESY correlations between H_3-15^1–OCH_3/H_2-17^1 and H-15^2–OCH_3/H-17 confirmed that H-17, H-18^1, and H-15^2–OCH_3 occupy phase-α positions, while H_2-17^1, H_2-17^2, H-18, and H_3-15^1–OCH_3 reside in phase-β positions. Thus, the structure of compound 7 was assigned and named atriplexophyll A.

Compound **8** was obtained as a greenish amorphous solid with molecular formula $C_{37}H_{38}N_4O_8$ determined by HRESIMS measurement. According to the identical molecular formula of **8** and 7 and the similar spectroscopic data of them, **8** and 7 were suggested to be stereoisomers. The ^1H and ^{13}C NMR spectra (Table 3) supported similarities between compounds **8** and 7, except for differences in the chemical shift of H_3-15^1–OCH_3 (7: δ_H 3.89; **8**: δ_H 3.54). The upfield shift of H_3-15^1–OCH_3 and the absence of the NOESY correlation (Fig. 6) between H_3-15^1–OCH_3/H-17^1 indicated that H_3-15^1–OCH_3 was in α-orientation. Thus, the structure of compound **8** was assigned and named atriplexophyll B.

Through a comparison of the experiments and reported spectroscopic data (UV, IR, NMR, and MS), 13 known compounds were identified to be saikogenin F (**9**),[35] corchorusin B (**10**),[36] c3-*O*-((β-D-glucopyranosyl-(1->2))-β-D-galactopyranosyl)-saikogenin F (**11**),[37] methyl pheophorbide b (**12**),[38] 13^2(*S*)-hydroxypheophorbide a methyl ester (**13**),[39] lutein (**14**),[40] paprazine (**15**),[41] (*E*)-*N*-feruloyltyramine (**16**),[41] *N*-*trans*-feruloyl-3-*O*-methyldopamine (**17**),[42] 1-(9*H*-β-carbolin-1-yl)-ethanone (**18**),[43] methyl 9*H*-pyrido[3,4-*b*]indole-1-carboxylate (**19**),[44] isorhamnetin (**20**),[45] and 5,7,4′-trihydroxy-4-styrylcoumarin (**21**).[46]

Approximately 300 species of the genus *Atriplex* have been identified worldwide, and triterpenoids are the primary class of isolated compounds to data. With FBMN-guided results, nine triterpenoids were isolated from the whole plant of *A. maximowicziana*. Our results align with previous findings, providing additional evidence that enhances the chemotaxonomic understanding of the genus *Atriplex* species. Besides, this study firstly represents the isolation of oleanane-type triterpenoid-saponins (compounds **1–4**) bearing two glucose units from *Atriplex* species. In addition, the structural elucidation of sugar moieties within saponin-type triterpenoids benefited from the application of 1D selective TOCSY NMR experiments. This technique enabled the accurate determination of glycosidic proton connectivities. It was particularly effective in distinguishing overlapping sugar resonances, thereby enhancing the resolution of complex spin systems and improving the reliability of the structural assignments. Moreover, the chlorophyll derivatives, atriplexophyll A (7) and atriplexophyll B (**8**) were successfully separated for the first time. Their detailed physical properties and NMR data are presented, providing a valuable reference for future studies of chlorophyll derivatives.

Anti-CRC effects of compounds isolated from *A. maximowicziana*

This study examines the anti-CRC effects of 18 isolated compounds **1–17** and **19** in human colorectal cancer cell lines HT-29 and HCT-116, respectively. As shown in Table 4, compounds **5–11** at the concentration of 20 μM showed inhibitory effects on the cell viability of HT-29 cells. Compounds 7, **8**, **16**, and **19** exhibited inhibition activity of cell viability toward HCT-116 cells at the concentration of 20 μM.

Two of the most potent cell viability inhibition compounds (7 and **8**) were further evaluated their IC_{50} values of anti-CRC activity (Fig. S66). As illustrated in Table 4, atriplexophyll A (7) exhibited the most potent anti-CRC activity by suppressing HT-29 cell viability (IC_{50} = 0.33 ± 0.02 μM) and HCT-116 cell viability (IC_{50} = 0.14 ± 0.03 μM), respectively. Besides, atriplexophyll B (**8**) showed cell viability inhibitory effects on HT-29 cells (IC_{50} = 8.81 ± 0.74 μM) and HCT-116 cells (IC_{50} = 7.95 ± 2.93 μM), respectively. Notably, both compounds showed no detectable cytotoxic effects on non-cancerous IEC-6 (intestinal epithelial) and 3T3-L1 (preadipocyte fibroblast) cell lines (Table 5). This selective activity suggests that compounds 7 and **8** exert their cytotoxic effects preferentially on malignant cells, minimizing off-target toxicity to normal tissues.

Tetrapyrroles molecular structures exist mainly as chlorophylls in plants. Chlorophyll-derived compounds have previously been shown to exhibit promising anticancer properties.[47] For example, chlorophyll a has been reported to have antiproliferative effects on human pancreatic cancer cells by mediated changes in the redox status.[48] Another type of chlorophyll, chlorophyllin, has been reported to deactivate ERKs to inhibit cell proliferation of MCF-7 human breast cancer cell lines.[49] Among the 18 tested compounds (compounds **1–17** and **19**) in the current study, only chlorophyll compounds 7 and **8** significantly inhibited cell viability in HT-29 and HCT-116 cells. The other two known chlorophylls, methyl pheophorbide b (**12**) and 13^2(*S*)-hydroxypheophorbide a methyl ester (**13**), did not

Table 4 Effects of compounds on cell viability in HT-29 and HCT-116 cells

	HT-29		HCT-116	
Compound	[a]Cell viability (%)	[b]IC_{50} (μM)	[a]Cell viability (%)	[b]IC_{50} (μM)
DMSO	100.00 ± 0.71	—	100.00 ± 2.35	—
1	88.67 ± 1.47	>20	92.50 ± 2.01	>20
2	93.35 ± 0.81	>20	87.60 ± 1.45	>20
3	88.68 ± 1.28	>20	84.23 ± 2.56	>20
4	91.44 ± 0.91	>20	93.73 ± 0.81	>20
5	76.49 ± 3.53***	>20	110.75 ± 2.20	>20
6	87.22 ± 2.12*	>20	99.82 ± 5.86	>20
7	24.89 ± 2.86***	0.33 ± 0.02	21.80 ± 0.37***	0.14 ± 0.03
8	19.76 ± 2.80***	8.81 ± 0.74	34.95 ± 1.44***	7.95 ± 2.93
9	75.04 ± 3.32***	>20	112.04 ± 8.05	>20
10	81.59 ± 1.71***	>20	93.66 ± 3.48	>20
11	86.42 ± 2.24**	>20	91.10 ± 3.84	>20
12	94.10 ± 2.90	>20	93.59 ± 8.41	>20
13	92.15 ± 2.38	>20	93.35 ± 3.21	>20
14	97.65 ± 2.00	>20	101.25 ± 4.46	>20
15	93.15 ± 1.70	>20	86.70 ± 2.73	>20
16	94.55 ± 2.51	>20	81.97 ± 2.12*	>20
17	99.87 ± 0.68	>20	85.13 ± 4.65	>20
19	94.25 ± 2.41	>20	69.89 ± 3.31***	>20

[a] Cell viability at 20 μM for 48 h. Results are presented as mean ± S.E.M. ($n = 3$) and used to calculate IC_{50} values. *$p < 0.05$; **$p < 0.01$; ***$p < 0.001$ compared with the DMSO group. [b] Concentration necessary for 50% inhibition (IC_{50}).

Table 5 Effects of compounds on cell viability in IEC-6 and 3T3-L1 cells

	IEC-6		3T3-L1	
Compound	[a]Cell viability (%)	[b]IC_{50} (μM)	[a]Cell viability (%)	[b]IC_{50} (μM)
DMSO	100.00 ± 0.32	—	100.00 ± 1.90	—
7	98.39 ± 1.30	—	99.12 ± 0.16	—
8	99.30 ± 0.38	—	96.96 ± 0.46	—

[a] Cell viability at 20 μM for 48 h. Results are presented as mean ± S.E.M. ($n = 3$). ***$p < 0.001$ compared with the DMSO group. [b] Concentration necessary for 50% inhibition (IC_{50}).

show such effects. In a previous study, compounds **7** and **8** were reported as a mixture under the name 15^2-methoxy lactone pheophorbide-b methyl ester.[34] That publication only disclosed the structural elucidation; no biological activity was investigated or reported.[34] To our knowledge, this is the first report to describe the biological activity of these compounds. Our findings indicated that not all chlorophyll-derived compounds exhibit anticancer activity. Nonetheless, this study highlights that chlorophyll-*b* type compounds containing a pyran ring show promising potential for further investigation in developing herbal medicines and therapeutic agents against human colorectal cancer. Moreover, chlorophyll derivatives have been reported to exert cancer prevention activity,[50] overcome multidrug resistance,[51] and serve as photosensitizers for the photodynamic cancer therapy.[52] Among them, pheophorbide a exhibits potent antiproliferative activity against various cancer cell lines[53] and strong photosensitizing cytotoxicity in HT-29 colon tumor cells (IC_{50}: 0.4 μM).[54] For comparison, our isolate atriplexophyll A (**7**) showed comparable potency against HT-29 cells (IC_{50}: 0.33 ± 0.02 μM). In HCT-116 cells, inhibition has also been reported for pheophorbide a[53] and chlorophyllin (IC_{50}: 20.2 ± 0.9 μM),[55] whereas atriplexophyll A (**7**) and atriplexophyll B (**8**) displayed IC_{50} values of 0.14 ± 0.03 μM and 7.95 ± 2.93 μM, respectively. These comparisons underscore noteworthy anti-CRC potential of atriplexophyll A (**7**) and atriplexophyll B (**8**).

An in-depth discussion of the structure–activity relationships (SAR) among the tested compounds is also provided. Among the four chlorophyll derivatives (compounds **7**, **8**, **12**, and **13**) evaluated for anti-CRC activity, only compounds **7** and **8** exhibited significant activity, suggesting that the presence of a pyran ring may enhance anti-CRC potential. Furthermore, compound **7** demonstrated stronger anti-CRC activity compared to compound **8**, underscoring the critical influence of the stereochemical orientation of the OCH_3 substituent at position C-15^1 on biological efficacy.

Conclusions

This study represents the first systematic phytochemical investigation of *A. maximowicziana*, integrating FBMN, and bioactivity-guided fractionation. A total of 21 compounds were

identified from *A. maximowicziana via* FBMN-guided phytochemical investigation, comprising eight previously undescribed metabolites and thirteen known constituents. The stereoisomeric chlorophylls, compounds 7 and **8**, were firstly separated and provided their NMR data. Additionally, eighteen compounds isolated from *A. maximowicziana* were evaluated for anticancer activity against human colorectal cancer cell lines HT-29 and HCT-116. This is the first report on the anti-CRC activity of pyran ring-type chlorophylls and illustrates the potential of atriplexophylls A (7) and B (**8**) to develop therapeutics against human colorectal cancer. These findings expand the bioactivity landscape of chlorophyll-derived natural products and provide a rationale for further exploration of chlorophyll-*b*-type with pyran ring compounds in anticancer drug discovery. Although triterpenoid-saponins and triterpenoid constituents did not exhibit potent cytotoxicity in this study, it expanded the chemotaxonomic understanding of the genus *Atriplex*. Furthermore, the use of 1D selective TOCSY NMR proved instrumental in resolving the sugar proton connectivities in complex saponin structures, reinforcing the importance of advanced NMR methods in natural product structure elucidation. In an overview, this study enriches the phytochemical profile of *A. maximowicziana* and identifies chlorophyll-*b*-type compounds with promising CRC-selective activity, providing substantive evidence for potential use in developing herbal medicines and drugs for human colorectal cancer.

Author contributions

Conceptualization, H.-C. W. and T.-H. L.; data curation, H.-C. W.; formal analysis, A. G., P.-J. C., Y.-F. C., and H.-C. W.; funding acquisition, H.-C. W and T.-H. L.; investigation, A. G., P.-J. C. and Y.-F. C.; methodology, P.-J. C. and H.-C. W.; project administration, H.-C. W.; resources, H.-C. W.; supervision, H.-C. W.; validation, A. G., P.-J. C., and H.-C. W.; visualization, A. G. and P.-J. C.; writing – original draft, A. G.; writing – review and editing, P.-J. C. and H.-C. W.

Conflicts of interest

There are no conflicts to declare.

Data availability

The data supporting this study are available in the supplementary information (SI). Supplementary information: isolation flow chart of compounds **1–21**, NMR and MS spectra of compounds **1–8**, and cell viability results of compounds 7 and **8**. See DOI: **https://doi.org/10.1039/d5ra06325f**.

Acknowledgements

The authors appreciate Dr Shing-Jong Huang of the Instrumentation Center, National Taiwan University, and Ms Chyi-Jia Wang of the Center for Research Resources and Development at Kaohsiung Medical University for providing high-quality NMR spectra. The authors also acknowledge the mass spectrometry technical research services from Consortia of Key Technologies and Instrumentation Center, National Taiwan University and from the Agricultural Biotechnology Research Center, Academia Sinica. This research was funded by grants (NSTC 112-2320-B-038-015-MY3, NSTC 112-2320-B-037-036-MY3 to H.-C. W. and NSTC 113-2320-B-002-050-MY3 to T.-H. L.) from the National Science and Technology Council, R.O.C. (Taiwan), supported by a grant from the Kaohsiung Medical University Research Foundation (KMU-Q114003) and by Kaohsiung Medical University Research Grant (KMU-TB114005).

References

1 M. N. Grigore and C. Toma, in *Handbook of Halophytes: from Molecules to Ecosystems towards Biosaline Agriculture*, ed. M. N. Grigore, Springer Cham, Switzerland, 2021, pp. 1079–1221.
2 V. de la Fuente, I. Sánchez-Gavilán, E. Ramírez, L. Rufo and D. Sánchez-Mata, in *Handbook of Halophytes: from Molecules to Ecosystems towards Biosaline Agriculture*, ed. M. N. Grigore, Springer, Cham, Switzerland, 2021, pp. 1223–1258.
3 O. A. Rozentsvet, V. N. Nesterov and E. S. Bogdanova, *Russ. J. Plant Physiol.*, 2017, **64**, 464–477.
4 Z. A. Reshi, W. Ahmad, A. S. Lukatkin and S. B. Javed, *Metabolites*, 2023, **13**, 895–917.
5 J. Lee, J. H. Song, S. H. Mun, H. J. Ko, S. Um and S. H. Kim, *Mar. Drugs*, 2024, **22**, 524–536.
6 M. M. Rahman, M. J. Kim, J. H. Kim, S. H. Kim, H. K. Go, M. H. Kweon and D. H. Kim, *Pharm. Biol.*, 2018, **56**, 183–191.
7 M. Roubi, A. Elbouzidi, M. Dalli, S.-E. Azizi, M. Aherkou, M. Taibi, B. El Guerrouj, M. Addi and N. Gseyra, *Sci. Afr.*, 2023, **22**, e01959–e01974.
8 H. A. Mohammed, A.-H. Emwas and R. A. Khan, *Int. J. Mol. Sci.*, 2023, **24**, 5171–5200.
9 B. Ali, R. Tabassum, N. Riaz, A. Yaqoob, T. Khatoon, R. B. Tareen, A. Jabbar, F. H. Nasim and M. Saleem, *J. Asian Nat. Prod. Res.*, 2015, **17**, 843–850.
10 D. Gođevac, J. Stanković, M. Novaković, B. Anđelković, Z. Dajić-Stevanović, M. Petrovic and M. Stanković, *J. Nat. Prod.*, 2015, **78**, 2198–2204.
11 B. S. Siddiqui, S. Ahmed and M. A. U. Khan, *Phytochem.*, 1994, **37**, 1123–1125.
12 A. Jabrane, H. Ben Jannet, T. Miyamoto, C. Tanaka, J. F. Mirjolet, O. Duchamp, F. Harzallah-Skhiri and M. A. Lacaille-Dubois, *Magn. Reson. Chem.*, 2011, **49**, 83–89.
13 A. Karim, I. Fatima, S. Hussain and A. Malik, *Helv. Chim. Acta*, 2011, **94**, 528–533.
14 A. I. Elshamy, T. A. Mohamed, M. Suenaga, M. Noji, A. Umeyama, T. Efferth and M. E. F. Hegazy, *Phytochem. Lett.*, 2019, **34**, 74–78.
15 H. Y. Liu, in *Flora of Taiwan*, ed. T. C. Huang, National Science and Technology Council of Taiwan, Taiwan, 2nd ed. edn., 1996, vol. Volume 3, pp. 382–387.
16 C. H. Chang, G. Hsiao, S. W. Wang, J. Y. Yen, S. J. Huang, W. C. Chi and T. H. Lee, *Bot. Stud.*, 2023, **64**, 34–42.
17 M. Wang, J. J. Carver, V. V. Phelan, L. M. Sanchez, N. Garg, Y. Peng, D. D. Nguyen, J. Watrous, C. A. Kapono,

T. Luzzatto-Knaan, C. Porto, A. Bouslimani, A. V. Melnik, M. J. Meehan, W. T. Liu, M. Crusemann, P. D. Boudreau, E. Esquenazi, M. Sandoval-Calderon, R. D. Kersten, L. A. Pace, R. A. Quinn, K. R. Duncan, C. C. Hsu, D. J. Floros, R. G. Gavilan, K. Kleigrewe, T. Northen, R. J. Dutton, D. Parrot, E. E. Carlson, B. Aigle, C. F. Michelsen, L. Jelsbak, C. Sohlenkamp, P. Pevzner, A. Edlund, J. McLean, J. Piel, B. T. Murphy, L. Gerwick, C. C. Liaw, Y. L. Yang, H. U. Humpf, M. Maansson, R. A. Keyzers, A. C. Sims, A. R. Johnson, A. M. Sidebottom, B. E. Sedio, A. Klitgaard, C. B. Larson, C. A. B. P, D. Torres-Mendoza, D. J. Gonzalez, D. B. Silva, L. M. Marques, D. P. Demarque, E. Pociute, E. C. O'Neill, E. Briand, E. J. N. Helfrich, E. A. Granatosky, E. Glukhov, F. Ryffel, H. Houson, H. Mohimani, J. J. Kharbush, Y. Zeng, J. A. Vorholt, K. L. Kurita, P. Charusanti, K. L. McPhail, K. F. Nielsen, L. Vuong, M. Elfeki, M. F. Traxler, N. Engene, N. Koyama, O. B. Vining, R. Baric, R. R. Silva, S. J. Mascuch, S. Tomasi, S. Jenkins, V. Macherla, T. Hoffman, V. Agarwal, P. G. Williams, J. Dai, R. Neupane, J. Gurr, A. M. C. Rodriguez, A. Lamsa, C. Zhang, K. Dorrestein, B. M. Duggan, J. Almaliti, P. M. Allard, P. Phapale, L. F. Nothias, T. Alexandrov, M. Litaudon, J. L. Wolfender, J. E. Kyle, T. O. Metz, T. Peryea, D. T. Nguyen, D. VanLeer, P. Shinn, A. Jadhav, R. Muller, K. M. Waters, W. Shi, X. Liu, L. Zhang, R. Knight, P. R. Jensen, B. O. Palsson, K. Pogliano, R. G. Linington, M. Gutierrez, N. P. Lopes, W. H. Gerwick, B. S. Moore, P. C. Dorrestein and N. Bandeira, *Nat. Biotechnol.*, 2016, **34**, 828–837.

18 R. A. Quinn, L. F. Nothias, O. Vining, M. Meehan, E. Esquenazi and P. C. Dorrestein, *Trends Pharmacol. Sci.*, 2017, **38**, 143–154.

19 K. Duhrkop, M. Fleischauer, M. Ludwig, A. A. Aksenov, A. V. Melnik, M. Meusel, P. C. Dorrestein, J. Rousu and S. Bocker, *Nat. Methods*, 2019, **16**, 299–302.

20 H. W. Kim, M. Wang, C. A. Leber, L. F. Nothias, R. Reher, K. B. Kang, J. J. J. van der Hooft, P. C. Dorrestein, W. H. Gerwick and G. W. Cottrell, *J. Nat. Prod.*, 2021, **84**, 2795–2807.

21 Y. Djoumbou Feunang, R. Eisner, C. Knox, L. Chepelev, J. Hastings, G. Owen, E. Fahy, C. Steinbeck, S. Subramanian, E. Bolton, R. Greiner and D. S. Wishart, *J. Cheminf.*, 2016, **8**, 61–80.

22 L. F. Nothias, D. Petras, R. Schmid, K. Duhrkop, J. Rainer, A. Sarvepalli, I. Protsyuk, M. Ernst, H. Tsugawa, M. Fleischauer, F. Aicheler, A. A. Aksenov, O. Alka, P. M. Allard, A. Barsch, X. Cachet, A. M. Caraballo-Rodriguez, R. R. Da Silva, T. Dang, N. Garg, J. M. Gauglitz, A. Gurevich, G. Isaac, A. K. Jarmusch, Z. Kamenik, K. B. Kang, N. Kessler, I. Koester, A. Korf, A. Le Gouellec, M. Ludwig, H. C. Martin, L. I. McCall, J. McSayles, S. W. Meyer, H. Mohimani, M. Morsy, O. Moyne, S. Neumann, H. Neuweger, N. H. Nguyen, M. Nothias-Esposito, J. Paolini, V. V. Phelan, T. Pluskal, R. A. Quinn, S. Rogers, B. Shrestha, A. Tripathi, J. J. J. van der Hooft, F. Vargas, K. C. Weldon, M. Witting, H. Yang, Z. Zhang, F. Zubeil, O. Kohlbacher, S. Bocker, T. Alexandrov, N. Bandeira, M. Wang and P. C. Dorrestein, *Nat. Methods*, 2020, **17**, 905–908.

23 H. Sung, J. Ferlay, R. L. Siegel, M. Laversanne, I. Soerjomataram, A. Jemal and F. Bray, *CA: Cancer J. Clin.*, 2021, **71**, 209–249.

24 M. Arnold, M. S. Sierra, M. Laversanne, I. Soerjomataram, A. Jemal and F. Bray, *Gut*, 2017, **66**, 683–691.

25 E. Van Cutsem, A. Cervantes, R. Adam, A. Sobrero, J. H. Van Krieken, D. Aderka, E. A. Aguilar, A. Bardelli, A. Benson and G. Bodoky, *Ann. Oncol.*, 2016, **27**, 1386–1422.

26 D. J. Newman and G. M. Cragg, *J. Nat. Prod.*, 2020, **83**, 770–803.

27 R. H. Shoemaker, *Nat. Rev. Cancer*, 2006, **6**, 813–823.

28 A. Olejniczak, M. Szaryńska and Z. Kmieć, *Int. J. Oncol.*, 2018, **52**, 599–612.

29 M. C. Chambers, B. Maclean, R. Burke, D. Amodei, D. L. Ruderman, S. Neumann, L. Gatto, B. Fischer, B. Pratt, J. Egertson, K. Hoff, D. Kessner, N. Tasman, N. Shulman, B. Frewen, T. A. Baker, M. Y. Brusniak, C. Paulse, D. Creasy, L. Flashner, K. Kani, C. Moulding, S. L. Seymour, L. M. Nuwaysir, B. Lefebvre, F. Kuhlmann, J. Roark, P. Rainer, S. Detlev, T. Hemenway, A. Huhmer, J. Langridge, B. Connolly, T. Chadick, K. Holly, J. Eckels, E. W. Deutsch, R. L. Moritz, J. E. Katz, D. B. Agus, M. MacCoss, D. L. Tabb and P. Mallick, *Nat. Biotechnol.*, 2012, **30**, 918–920.

30 O. D. Myers, S. J. Sumner, S. Li, S. Barnes and X. Du, *Anal. Chem.*, 2017, **89**, 8696–8703.

31 T. D. Viet, T. D. Xuan and L. H. Anh, *Molecules*, 2021, **26**, 7248–7261.

32 P. Rubiano-Buitrago, R. A. White, A. P. Hastings, F. C. Schroeder, A. A. Agrawal and C. Duplais, *J. Nat. Prod.*, 2024, **88**, 49–57.

33 X. Nan, S. Ya-Nan, X. Zhong, C. Yue, W. Li and J. Tian-Zhu, *Chin. J. Nat. Med.*, 2014, **12**, 305–308.

34 F. Adzhar Kamarulzaman, K. Shaari, A. Siong Hock Ho, N. Haji Lajis, S. Hwang Teo and H. Boon Lee, *Chem. Biodiversity*, 2011, **8**, 494–502.

35 K. Shimizu, S. Amagaya and Y. Ogihara, *Chem. Pharm. Bull.*, 1985, **33**, 3349–3355.

36 S. B. Mahato and B. C. Pal, *J. Chem. Soc., Perkin Trans.*, 1987, **1**, 629–634.

37 K. H. Shaker, K. Dockendorff and K. Seifert, *Z. Naturforsch. C*, 2003, **58**, 485–489.

38 Y. M. Chiang, H. K. Liu, J. M. Lo, S. h. Chien, Y. F. Chan, T. H. Lee, J. K. Su and Y. H. Kuo, *J. Chin. Chem. Soc.*, 2003, **50**, 161–166.

39 L. Ma and D. Dolphin, *J. Org. Chem.*, 1996, **61**, 2501–2510.

40 M. Afolayan, R. Srivedavyasasri, O. T. Asekun, O. B. Familoni and S. A. Ross, *Nat. Prod. Res.*, 2019, **33**, 287–291.

41 S. Achanta, V. Liautard, R. Paugh and M. G. Organ, *Chem. Eur. J.*, 2010, **16**, 12797–12800.

42 A. Othman, A. M. Sayed, Y. Amen and K. Shimizu, *RSC Adv.*, 2022, **12**, 18746–18758.

43 T. H. Trieu, J. Dong, Q. Zhang, B. Zheng, T. Z. Meng, X. Lu and X. X. Shi, *Eur. J. Org Chem.*, 2013, **2013**, 3271–3277.

44 S. Kolle and S. Batra, *Org. Biomol. Chem.*, 2015, **13**, 10376–10385.
45 L. M. Fernandes e Mendonça, A. B. Joshi, A. Bhandarkar, H. Joshi and S. Joshi, *Nat. Prod. Res.*, 2024, **38**, 768–772.
46 M. S. Abdel-Kader, *Planta Med.*, 2001, **67**, 388–390.
47 R. Dashwood, *Int. J. Oncol.*, 1997, **10**, 721–727.
48 K. Vaňková, I. Marková, J. Jašprová, A. Dvořák, I. Subhanová, J. Zelenka, I. Novosádová, J. Rasl, T. Vomastek and R. Sobotka, *Oxid. Med. Cell. Longev.*, 2018, **2018**, 4069167–4069178.
49 L. C.-M. Chiu, C. K.-L. Kong and V. E.-C. Ooi, *Int. J. Mol. Med.*, 2005, **16**, 735–740.
50 M. G. Ferruzzi and J. Blakeslee, *Nutr. Res.*, 2007, **27**, 1–12.
51 E. Wang, M. S. Braun and M. Wink, *Molecules*, 2019, **24**, 2968–2977.
52 W. T. Li, H. W. Tsao, Y. Y. Chen, S. W. Cheng and Y. C. Hsu, *Photochem. Photobiol. Sci.*, 2007, **6**, 1341–1348.
53 A. Saide, C. Lauritano and A. Ianora, *Mar. Drugs*, 2020, **18**, 257–268.
54 V. Rapozzi, M. Miculan and L. Xodo, *Cancer Biol. Ther.*, 2009, **8**, 1318–1327.
55 S. Sun, Y. Zhang, W. Xu, Y. Zhang, R. Yang, J. Guo, S. Guan, Q. Ma, K. Ma and J. Xu, *Antioxidants*, 2021, **10**, 1733–1745.